

## EARLY DETECTION OF ROTOR CORE BREAKAGE BASED ON PHASE CURRENT HARMONICS IN LOW-POWER ASYNCHRONOUS MOTORS (MCSA)

Toshtemirov Humoyun SHokir ugli

Tashkent State Transport University (Tashkent, Uzbekistan)

### Annotation

In this article, the problem of early detection of rotor rod breakage (Broken Rotor Bar, BRB) in low-power asynchronous motors (0.37-15 kW) is considered. The research is based on the Motor Current Signature Analysis (MCSA) - a diagnostic approach based on the stator phase current spectrum. The results of operational monitoring conducted in 2022-2025 showed an increase in the number of suspicious BRB cases from 2.0 to 5.3 per 100 motor bases, which confirms the relevance of this defect. Spectral analysis revealed the stable appearance of side-band components around the network frequency in the presence of BRB, whereas in a healthy state these components are not significantly observed. The study proposed a monitoring concept based on a portable current sensor (Hall/CT) and the MCSA algorithm. This approach allows for the early detection and organization of continuous monitoring in real operation, even under conditions of noise and variable load, characteristic of low-power engines.

### Keywords

Asynchronous motor; low-power motors; rotor stem breakage; MCSA; current spectrum; side-band components; portable diagnostics; monitoring.

### Introduction

Due to the widespread use of low-power asynchronous motors (0.37-15 kW) in pumps, fans, conveyors, and auxiliary mechanisms, their malfunction leads to unplanned stops and energy losses during the production process. According to the results of enterprise monitoring in 2022-2025, it was observed that "suspicious" cases of rotor rod fracture (Broken Rotor Bar, BRB) are increasing year by year: the indicator of 2.0 units/100 motor in 2022 increased to 5.3 units/100 motor by 2025. This indicates that the issue of early detection of BRB defects in the fleet of low-power engines is relevant both from a practical and economic point of view.[1]

The BRB defect causes electromechanical asymmetry in the rotor cage, resulting in pulsations in the electromagnetic moment and an increase in slip. Such processes are directly reflected in the current signals, i.e., the development of BRB is characterized by the appearance of amplitude-modulation and spectral "side-band" components in the stator phase current. Therefore, in this study, a diagnostic approach based on Motor Current Signature Analysis (MCSA) - stator phase current harmonics (spectrum) was chosen for the early detection of BRB.



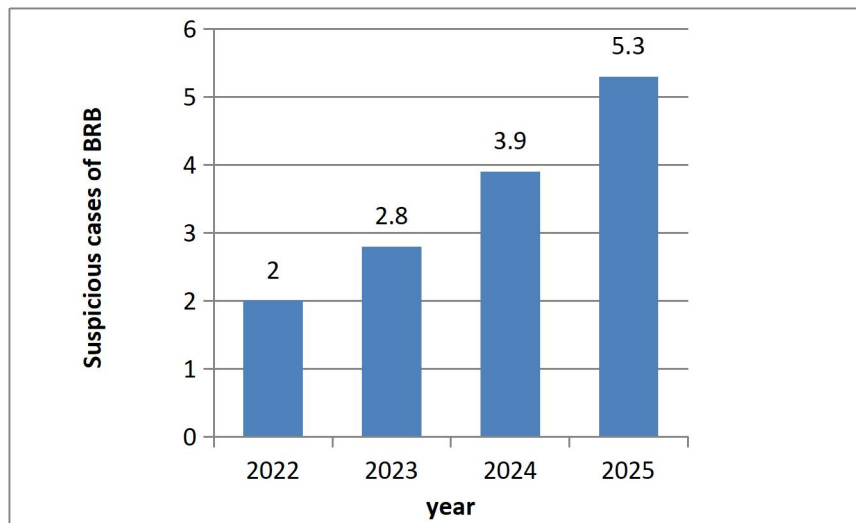


**Figure 1 (trend): 2022-2025 Growth of suspicious cases of BRB.**

## Materials and Methods

In this study, a method for early detection of rotor rod breakage (Broken Rotor Bar, BRB) in low-power asynchronous motors (0.37-15 kW) based on Motor Current Signature Analysis (MCSA) was developed. The approach is based on the physical regularity of the direct reflection of electromagnetic processes by stator phase currents and the formation of slip-dependent diagnostic components in the current spectrum when asymmetry occurs in the rotor cage. Experimental-monitoring data were recorded by current sensors (Hall or current transformer) in the form of three-phase current signals  $i_a(t)$ ,  $i_b(t)$ ,  $i_c(t)$ ; the recorded signals were divided into time windows for further spectral analysis, and a resolution was provided that allows for the separation of the side-band components due to the frequency accuracy of the chosen ratio  $\Delta f=1/T_w$ .

The formation of spectral characteristics associated with the BRB is explained by the amplitude-modulation of the magnetic flux as a result of the asymmetry of the rotor circuit. This process leads to the appearance of side-band components in the stator current spectrum around the network frequency  $f_1$ . The basic diagnostic frequencies for BRB are represented within the classical MCSA as follows:

$$f_{ab}^{\pm} = f_1(1 \pm 2s) ;$$

where  $s$  is the slip, which is defined by the synchronous velocity  $n_s$  and the rotor velocity  $n_r$ :

$$s = \frac{n_s - n_r}{n_s}, \quad s = \frac{120f_1}{p} ;$$

$p$  - number of poles. Since in practical conditions the components of the BRB may not be limited only to the first order, high-order sidebands are also taken into account:

$$f_{ab,k}^{\pm} = f_1(1 \pm 2ks) , \quad k=1,2,...$$

However, since noise and load vibrations can be strong in low-power engines, in terms of diagnostic stability, components typically around  $k=1$  were chosen as a priority indicator.

The measured current signals underwent preliminary processing to prepare for spectral analysis: the average value (DC offset) was removed and normalization was performed. In order to reduce the phase imbalance and measurement noise in low-power motors, three-phase currents



were converted to  $\alpha\beta$  coordinates through a Clarke transformer, and an amplitude-invariant signal was formed: [2], [3].

$$\begin{bmatrix} i_\alpha \\ i_\beta \end{bmatrix} = \frac{1}{3} \begin{bmatrix} 1 & -\frac{1}{2} & -\frac{1}{2} \\ 0 & \frac{\sqrt{3}}{2} & -\frac{\sqrt{3}}{2} \end{bmatrix} \begin{bmatrix} i_a \\ i_b \\ i_c \end{bmatrix}, \quad i_{\alpha\beta}(t) = \sqrt{i_a^2(t) + i_\beta^2(t)}.$$

At the next stage, to assess the spectral composition, the amplitude spectrum  $X(f)$  was obtained using the Fast Fourier Transform (FFT) with a Hanning window:

$$X(f) = \left[ \sum_{n=0}^{N-1} x[n] w[n] e^{-j2\pi fn/N} \right],$$

where  $x[n]$  is the phase current or  $i_{\alpha\beta}$  signal,  $w[n]$  is the mirroring function. It is also envisaged to use time-frequency analysis (TFA) to determine the displacement of the side belt components in modes in which the change in load over time is observed:

$$X(f) = \left[ \sum_{n=0}^{N-1} x[n] w[n-t] e^{-j2\pi fn/N} \right].$$

Since the frequency of the BRB components depends on the slip, a "slip-tracking" approach was implemented under variable load conditions: a lateral band peak detected around  $f_1$  was estimated by slip sensorless via fpeak:

$$s = \frac{1}{2} \left| \frac{f_{\text{peak}} - f_1}{f_1} \right|.$$

Then, the amplitudes of the lateral bands were isolated in a narrow range of around  $f_1$  ( $1\pm2s$ ), and diagnostic indices were formed for a quantitative assessment of the condition of the PPR. As a classic and understandable indicator, the ratio of the amplitudes of the sideband to the main component was adopted:

$$K_{\text{RB}} = \frac{A(f_1(1-2s)) + A(f_1(1+2s))}{A(f_1)}.$$

To increase noise immunity, the ratio of the spectrum energy in the sideband range to the range of the main component was additionally used:

$$K_E = \frac{\sum_{f \in \Omega_{\text{sb}}} |X(f)|^2}{\sum_{f \in \Omega_1} |X(f)|^2},$$

where  $\Omega_{\text{ab}}$  is the range  $\pm\delta$  around  $f_1$  ( $1\pm2s$ ),  $\Omega_1$  is the range around  $f_1$ .

The decision-making mechanism was built on the basis of basic statistics collected on healthy motors: the threshold value was determined based on the average value of the indices in a healthy state  $\mu_0$  and the variance  $\sigma_0$ : [2], [3], [4].

$$\Theta = \mu_0 + \lambda \sigma_0,$$

and the CRP is detected as follows:

$$\text{BRB shubhali} \Leftrightarrow K_{\text{RB}} > \Theta \text{ (yoki } K_E > \Theta).$$

## Results

The spectral results clearly confirmed the "signature" characteristic of the BRB case. In a healthy state, the main component is dominant in the spectrum, and no additional strong peaks are observed around the network frequency. In the case of BRB, two symmetrical side peaks ("side-band" components) around the network frequency are significantly amplified. This phenomenon is explained by the modulation of the electromagnetic field as a result of asymmetry in the rotor cage, and it is this feature that serves as the main practical criterion for diagnosing BRD for MCSA. An important aspect is that this spectral characteristic is not



"dependent" on the power value - even in engines in the range of 0.37-15 kW, if there is a rotor core breakage, the appearance of such side-belt components is expected; the difference is mainly in their amplitude and stability (load vibration, noise, operating mode effect). Figure 2 (spectrum): Difference between the state spectrum of the healthy state and the state spectrum of the BRD (side-band components). [4], [5].

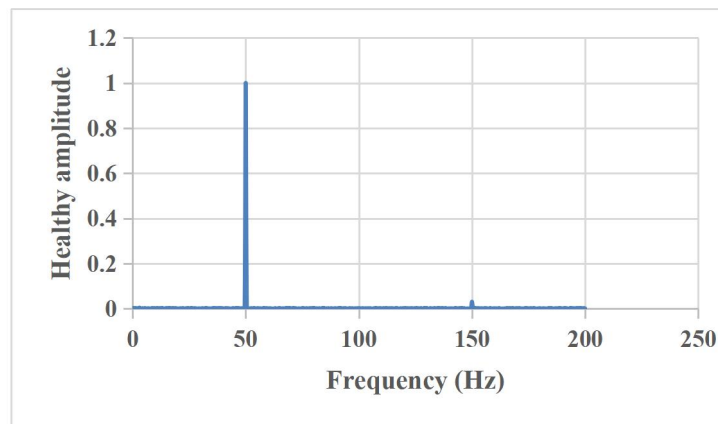


**Figure 2 (spectrum): Difference between the state spectrum of the healthy state and the state spectrum of the BRD (side-band components).**

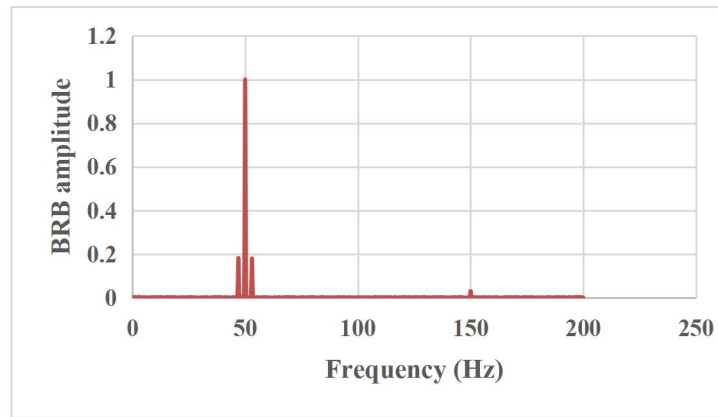


**Figure 3 (spectrum): Difference between the unhealthy state and the RRD state spectrum (side-band components).**

To demonstrate the possibility of applying the results in real operation, the diagnostic chain was linked to the concept of portable monitoring. Using a Hall/CT current sensor connected to a three-phase cable via a clip, the phase current signal is obtained, digitized, and spectral analysis is performed in the device's internal computing module. After identifying the components specific to BRB in the spectrum, the system displays the final conclusion to the user as "Healthy / Suspicious BRB" and records the result in the log. This approach allows for the establishment of diagnostics even outside laboratory conditions: that is, in the fleet of low-power engines, the examination will not be "one-time," but will transition to a permanent monitoring format.





**Figure 4 (device): View (location) of a portable MCSA device where current sensors are connected to the motor cable.**

The block diagram of the algorithm clearly shows the resulting process: a current signal is obtained, noise exposure is reduced, the spectrum is calculated, an assessment is performed according to the BRB characteristic, and the final decision is connected to the monitoring report. Due to this, the 2022-2025 annual trend (Fig. 1) is formed not as a random observation, but as a result of monitoring, collected on the basis of a unified diagnostic logic. [5], [6].

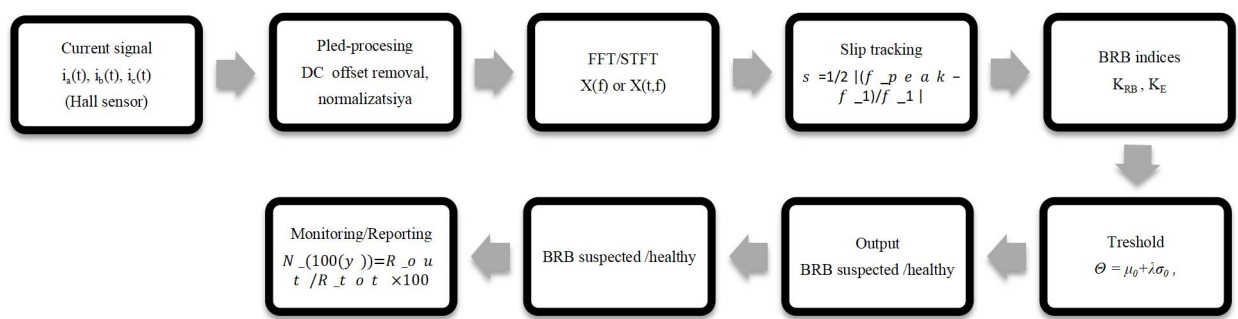


**Figure 5 (algorithm): Block diagram based on MCSA for early detection of RRD.**

Monitoring in 2022-2025 showed an increase in suspicious cases of BRM; In the presence of the BRB, with the appearance of sideband peaks in the current spectrum around 50 Hz, it is separated from the healthy state; the portable current sensor and algorithm allow organizing early warning monitoring in real operation based on this sign.

## Conclusion

This paper investigated the early detection of broken rotor bars (BRB) in low-power induction motors (0.37–15 kW) using Motor Current Signature Analysis (MCSA). Monitoring results collected over the 2022–2025 period revealed a steady increase in suspected BRB cases, rising from 2.0 to 5.3 per 100 motors, which clearly indicates the growing operational relevance of this fault in low-power motor fleets. Spectral analysis confirmed that the presence of BRB is characterized by the amplification of stable sideband components around the supply frequency, while such components remain insignificant under healthy operating conditions, validating the use of MCSA as a practical diagnostic approach for BRB detection.

From an application perspective, a portable monitoring concept based on clamp-on Hall/CT current sensors combined with an embedded spectral analysis algorithm was proposed. This solution enables continuous condition monitoring of induction motors directly under real operating conditions, without the need for intrusive measurements or additional mechanical sensors. The results further demonstrate that, despite the low signal-to-noise ratio and load



variability typical of low-power motors, BRB-related spectral features can be reliably extracted and tracked for early fault identification.

## References

1. Thomson, W. T., & Fenger, M. (2001). Current signature analysis to detect induction motor faults. *IEEE Industry Applications Magazine*, 7(4), 26–34.
2. Benbouzid, M. E. H. (2000). A review of induction motors signature analysis as a medium for faults detection. *IEEE Transactions on Industrial Electronics*, 47(5), 984–993.
3. Bellini, A., Filippetti, F., Franceschini, G., & Tassoni, C. (2008). Closed-loop control impact on the diagnosis of induction motors faults. *IEEE Transactions on Industry Applications*, 44(5), 1539–1547.
4. Nandi, S., Toliyat, H. A., & Li, X. (2005). Condition monitoring and fault diagnosis of electrical motors - A review. *IEEE Transactions on Energy Conversion*, 20(4), 719–729.
5. Antonino-Daviu, J. A., Riera-Guasp, M., Roger-Folch, J., & Martinez-Gimenez, F. (2006). Application and optimization of the discrete wavelet transform for the detection of broken rotor bars in induction machines. *Applied and Computational Harmonic Analysis*, 21(2), 268–279.
6. Siddique, A., Yadava, G. S., & Singh, B. (2005). A review of stator fault monitoring techniques of induction motors. *IEEE Transactions on Energy Conversion*, 20(1), 106–114.

